Yeast pericentrin/Spc110 contains multiple domains required for tethering the γ-tubulin complex to the centrosome

Annabel Alonso[a], Amy Fabritius[a], Courtney Ozzello[b], Mike Andreas[c], Dima Klenchin[d], Ivan Rayment[e], and Mark Winey[a,*]

[a]Department of Molecular and Cellular Biology, University of California, Davis, Davis, CA 95616; [b]The Boulder Laboratory for 3D Electron Microscopy of Cells, Department of Molecular, Cellular, and Developmental Biology, University of Colorado–Boulder, Boulder, CO 80309; [c]Department of Biomedical Engineering, University of Michigan, Ann Arbor, MI 48109; [d]Department of Pathology and Laboratory Medicine and [e]Department of Biochemistry, University of Wisconsin–Madison, Madison, WI 53706

ABSTRACT **The *Saccharomyces cerevisiae* spindle pole body (SPB) serves as the sole microtubule-organizing center of the cell, nucleating both cytoplasmic and nuclear microtubules. Yeast pericentrin, Spc110, binds to and activates the γ-tubulin complex via its N terminus, allowing nuclear microtubule polymerization to occur. The Spc110 C terminus links the γ-tubulin complex to the central plaque of the SPB by binding to Spc42, Spc29, and calmodulin (Cmd1). Here, we show that overexpression of the C terminus of Spc110 is toxic to cells and correlates with its localization to the SPB. Spc110 domains that are required for SPB localization and toxicity include its Spc42-, Spc29-, and Cmd1-binding sites. Overexpression of the Spc110 C terminus induces SPB defects and disrupts microtubule organization in both cycling and G2/M arrested cells. Notably, the two mitotic SPBs are affected in an asymmetric manner such that one SPB appears to be pulled away from the nucleus toward the cortex but remains attached via a thread of nuclear envelope. This SPB also contains relatively fewer microtubules and less endogenous Spc110. Our data suggest that overexpression of the Spc110 C terminus acts as a dominant-negative mutant that titrates endogenous Spc110 from the SPB causing spindle defects.**

Monitoring Editor
Kerry Bloom
University of North Carolina, Chapel Hill

Received: Feb 26, 2020
Revised: Apr 27, 2020
Accepted: May 1, 2020

INTRODUCTION

As the major microtubule-organizing centers (MTOCs) of the cell, centrosomes play a critical role in ensuring bipolar spindle assembly and accurate chromosome segregation. Centrosome duplication is cell cycle-regulated and is the first step in spindle formation (Rieder *et al.*, 2001; Azimzadeh and Bornens, 2007, reviewed in Strnad and Gonczy, 2008 and Bornens, 2012). Defects in centrosome duplication or function lead to chromosome instability, aneuploidy, and/or polyploidy, all of which are common in many types of cancers (Lengauer *et al.*, 1998; Pihan *et al.*, 1998; Ganem *et al.*, 2009). Despite the significant role played by centrosomes in chromosome segregation, the assembly mechanism and underlying functions of specific centrosome-associated proteins remain poorly understood.

In *Saccharomyces cerevisiae*, the spindle pole body (SPB) serves as the MTOC and is thus the functional equivalent of the centrosome (Jaspersen and Winey, 2004; Jones *et al.*, 2011; Kilmartin, 2014). The yeast SPB is made up of 18 components that assemble into a multilayered structure (Rout and Kilmartin, 1990; Knop and Schiebel, 1998; Adams and Kilmartin, 1999; O'Toole *et al.*, 1999; Ito *et al.*, 2001; Kilmartin, 2003; Jaspersen and Winey, 2004). The SPB remains embedded in the nuclear envelope throughout the cell cycle, since yeast cells undergo a closed mitosis (Byers and Goetsch, 1974, 1975; Winey *et al.*, 1995). Many of the key yeast

This article was published online ahead of print in MBoC in Press (http://www.molbiolcell.org/cgi/doi/10.1091/mbc.E20-02-0146) on May 6, 2020.

*Address correspondence to: Mark Winey (mwiney@ucdavis.edu).

Abbreviations used: Cmd1, Calmodulin; EM, electron microscopy; FRAP, fluorescence recovery after photobleaching; MTOC, microtubule-organizing center; NLS, nuclear localization sequence; PACT, pericentrin-AKAP450 centrosomal targeting; PBS, phosphate-buffered saline; SPB, spindle pole body.

SPB components and regulators have mammalian homologues, which makes budding yeast an ideal model system for the study of centrosomes (Knop *et al.*, 1997; Brachat *et al.*, 1998; Murphy *et al.*, 1998; Flory *et al.*, 2000, 2002; Gordon *et al.*, 2006; Kollman *et al.*, 2011; Ruthnick and Schiebel, 2016; Ito and Bettencourt-Dias, 2018). The most conserved protein complex in the SPB is the γ-tubulin complex, which is composed of Tub4 (γ-tubulin), Spc97, and Spc98. The γ-tubulin complex is anchored to the core of the SPB by binding to Spc72 in the cytoplasm and to Spc110 in the nucleus, thus nucleating cytoplasmic and nuclear microtubules, respectively (Knop *et al.*, 1997; Knop and Schiebel, 1997, 1998). The proteins that make up the γ-tubulin complex in yeast are analogous to the pericentriolar material of centrosomes, which is essential for microtubule nucleation in vertebrates (Mahen and Venkitaraman, 2012).

Spc110 is an essential component of the SPB that binds to and activates the γ-tubulin complex to nucleate the formation of nuclear microtubules (Kilmartin and Goh, 1996; Vinh *et al.*, 2002). The vertebrate Spc110 homolog, pericentrin (kendrin), is similarly required for the recruitment of the γ-tubulin complex to the centrosome (Oakley and Oakley, 1989; Doxsey *et al.*, 1994; Zheng *et al.*, 1995). Spc110 is composed of globular N and C terminal domains and a central coiled-coil domain. The coiled-coil domain forms a homodimer that spans the central and inner plaques of the SPB (Kilmartin *et al.*, 1993). The N terminus of Spc110 interacts with γ-tubulin complexes by binding to Spc98, a component of the γ-tubulin complex (Knop and Schiebel, 1997; Nguyen *et al.*, 1998). The conserved C terminal PACT (pericentrin-AKAP450 centrosomal targeting) domain of Spc110 interacts with the central plaque proteins Spc29, Spc42, and calmodulin (Cmd1) (Geiser *et al.*, 1993; Stirling *et al.*, 1994; Geier *et al.*, 1996; Kilmartin and Goh, 1996; Elliott *et al.*, 1999; Gillingham and Munro, 2000; Vinh *et al.*, 2002; Muller *et al.*, 2005). The PACT domain of pericentrin also binds Cmd1, similar to Spc110 (Geiser *et al.*, 1993; Stirling *et al.*, 1994; Gillingham and Munro, 2000). Although structural studies have investigated the interaction between the N terminal domain of Spc110 and the γ-tubulin complex, how the Spc110 C terminal domain interacts with the central plaque proteins remains largely unknown. Here, we show that each of the Spc29-, Spc42-, and Cmd1-binding domains in Spc110 are important for the localization of the Spc110 C terminus to the SPB. The PACT domain of pericentrin has also been shown to play a role in the recruitment of pericentrin to the centrosome (Gillingham and Munro, 2000). Interestingly, overexpression of the Spc110 C terminus (residues 741–944) results in lower levels of endogenous Spc110 at one of the two SPBs and in the other SPB being pulled away from the nucleus but remaining attached via a string of nuclear envelope. We hypothesize that the SPB is being drawn away from the nucleus due to a microtubule force imbalance on the spindle, which in turn leads to a cell cycle arrest.

RESULTS

The C terminus of Spc110 localizes to the SPB

Spc110 is known to bind to the SPB via its C terminal domain (Geiser *et al.*, 1993; Stirling *et al.*, 1994). To better define the Spc110 residues required for SPB localization, we generated a series of truncations of the Spc110 C terminus, including a Spc110 C terminal fragment consisting of residues 741–944 (Spc110 AA741–944). In previous studies, an Spc110 AA736–944 fragment was shown to be a stable domain (Muller *et al.*, 2005; Viswanath *et al.*, 2017). The Spc110 AA741–944 fragment contains a Cmd1-binding site (Muller *et al.*, 2005), a conserved domain that is thought to bind to Spc29, and a region that binds to Spc42 (Adams and Kilmartin, 1999; Elliott *et al.*, 1999). The constructs used in this study also contain a nuclear localization sequence (NLS), a fluorescent protein tag (GFP or YFP), 49 residues encoding the globular domain of the protein Gp7 from bacteriophage φ29 to allow the chimeric proteins to dimerize, and a *GAL1* promoter for inducible expression in galactose-containing medium and repression in glucose-containing medium (Flick and Johnston, 1990; Sibanda *et al.*, 2001; Morais *et al.*, 2003) (Figure 1A).

From the series of Spc110 C terminal truncations and internal deletion constructs, only the Spc110 AA741–944 C terminal fragment localized to the SPB (Figure 1B). The position of SPBs was identified based on the localization of the outer (cytoplasmic) plaque protein Nud1, which was tagged with Ruby2. Localization of the Spc110 AA741–944 C terminal fragment to the SPB was also visible when expressed at low levels in uninduced (-galactose) cells. Notably, we observed an unequal distribution of GFP signal, corresponding to the Spc110 AA741–944 C terminal fragment, between the two SPBs. Overexpression (+galactose) of the Spc110 AA741–944, Spc110 AA741–923, or Spc110 AA813–944 fragment led to the formation of additional GFP-marked signal distinct from that of the SPBs, while the other Spc110 fragments (Spc110 AA741-(Δ799–878)-944; Spc110 AA741-(Δ799–917)-944; Spc110 AA741–896; Spc110 AA799–856, Spc110 AA896–944; Spc110 AA741–813) showed diffuse nuclear localization (Supplemental Figure S1A). Herein, we use the term "aggregate" to refer to the GFP signal that was not associated with an SPB. It was previously observed that overexpression of Spc110p leads to the formation of spherical polymers in the nucleus (Kilmartin and Goh, 1996). In our studies, we found that the majority of SPB proteins we examined, with the exception of the two outer plaque proteins Nud1 and Spc72, were present in the aggregate (Supplemental Figure S1B). Our identification of Nud1 as an SPB component that did not localize to the aggregate allowed us to use it as the SPB marker in subsequent experiments. The overexpression of the Spc110 homolog in the fission yeast *Schizosaccharomyces Pombe*, Pcp1p, also produced SPB-like structures that contain other SPB components, similar to our observation (Flory *et al.*, 2002).

Overexpression of the Spc110 AA741–944 C terminal fragment induces a cell cycle arrest

Full-length Spc110 was shown previously to be nontoxic when overexpressed, whereas a similar construct containing an internal deletion, Spc110 AA1-(Δ216–600)-944 was toxic (Goh and Kilmartin, 1993). Here, we tested whether overexpression of the Spc110 AA741–944 C terminal fragment or of other C terminal fragments of Spc110 was toxic by plating cells harboring the construct on 2% galactose-containing medium (*GAL1* promoter activation) plates or on glucose-containing medium (*GAL1* promoter repression) as a negative control. Overexpression of the Spc110 AA741–944 C terminal fragment was toxic based on lack of growth in galactose-containing medium, whereas none of the other constructs tested were toxic (Figure 1C and Supplemental Figure S1C). Thus, the toxicity appeared to be correlated to the ability to localize to the SPB. Notably, the removal of only 21 amino acids from the C terminus of Spc110, corresponding to the Spc110 AA741–923 C terminal fragment, disrupted SPB localization and eliminated the toxic phenotype. Importantly, we demonstrated by immunoblot analysis that both the Spc110 AA741–944 and the Spc110 AA741–923 C terminal fragments showed similar protein expression levels (Supplemental Figure S2A). Similar to the previous overexpression study, we show that overexpression of full-length Spc110 is not toxic, and that

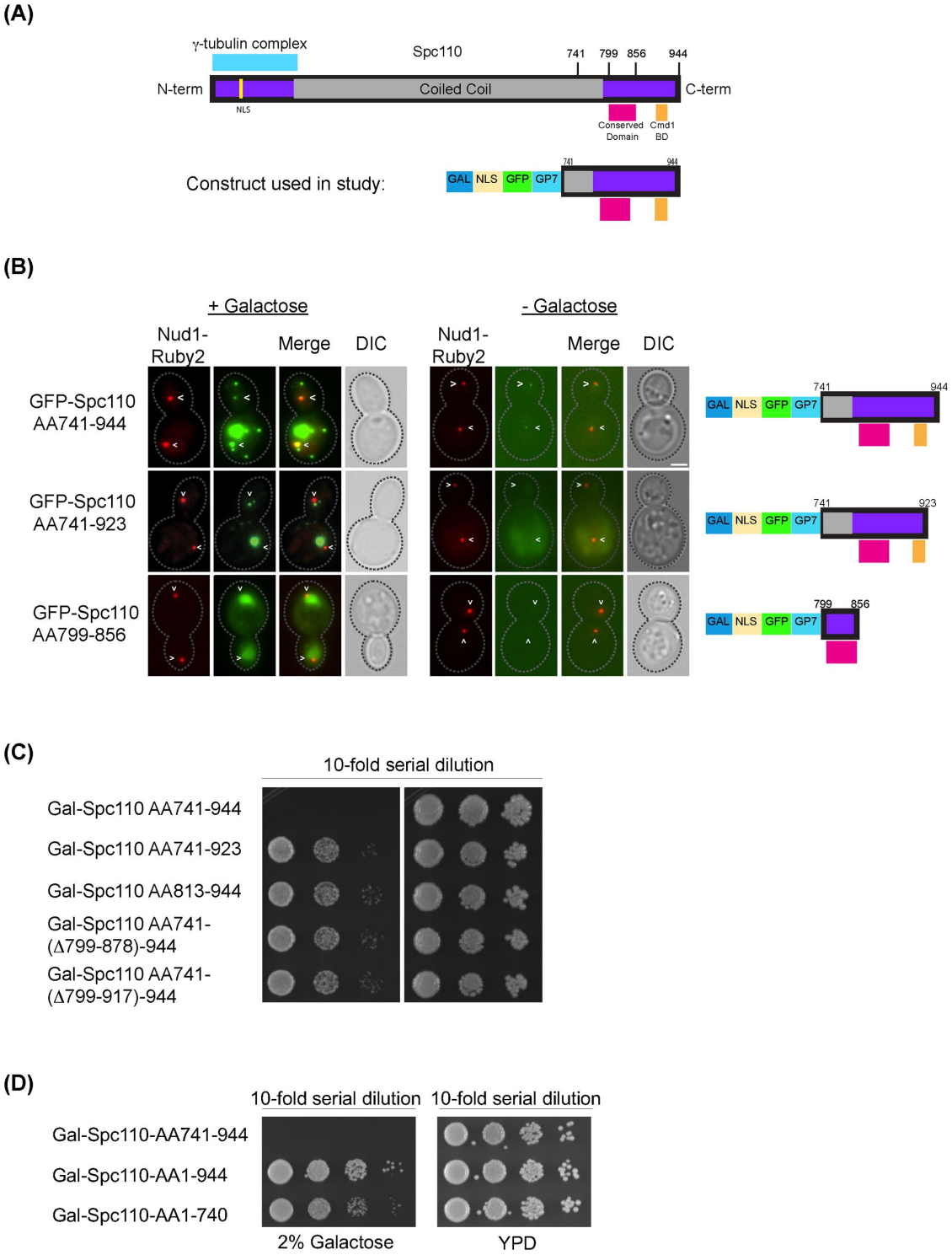

FIGURE 1: Overexpression of the Spc110 C terminus is toxic, and residues 741–944 are required for localization to the SPB. (A) Schematic of the Spc110 C terminal fragment clones. (B) Representative fluorescent images of SPB localization of GFP-tagged Spc110 C terminal fragments (green; pMW2661, Spc110 AA741–944; pMW2662, Spc110 AA741–923; pMW2966, Spc110 AA799–856) together with Nud1-Ruby2 (red). (C) Cells overexpressing the various Spc110 C terminal fragment constructs were spotted onto YEP + glucose (repression) and YEP + galactose (activation) plates. (D) Strains carrying the Spc110 C terminus, full length, and N terminal fragment were serial diluted onto galactose and glucose plates. Plates were incubated for 3 d at 30°C prior to imaging. Bar, 2 μm. Arrowhead = SPB.

overexpression of the Spc110 N terminus is also not toxic (Figure 1D); therefore, the toxicity is specific to the C terminus of Spc110. Based on these findings and for simplification, we refer to the Spc110 AA741–944 C terminal fragment as "Spc110 C-toxic" and to the Spc110 AA741–923 C terminal fragment as "Spc110 C-nontoxic" in subsequent experiments.

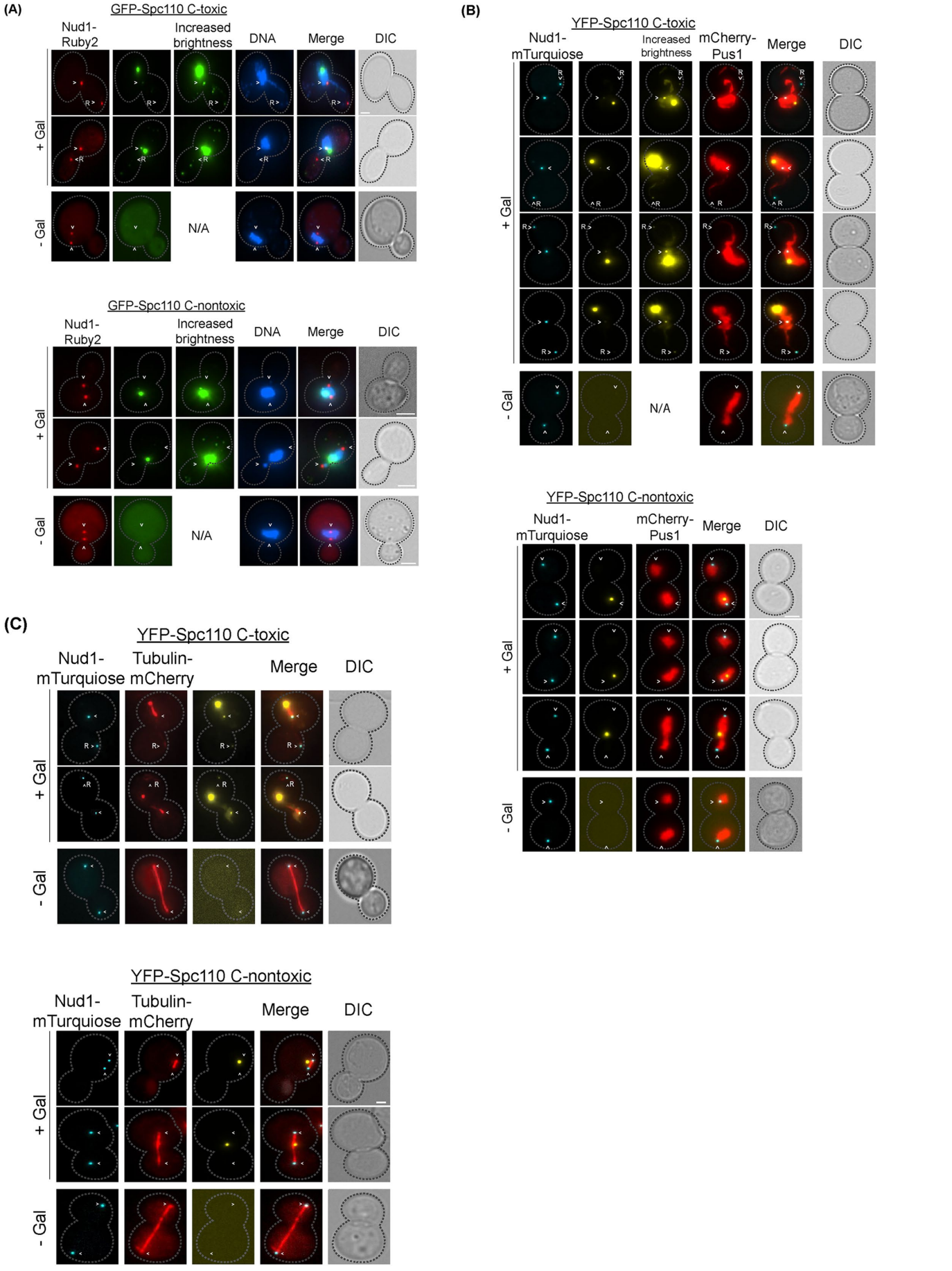
(A)
GFP-Spc110 C-toxic
Nud1-Ruby2
Increased brightness
DNA
Merge
DIC
+ Gal
- Gal
N/A
GFP-Spc110 C-nontoxic
Nud1-Ruby2
Increased brightness
DNA
Merge
DIC
+ Gal
- Gal
N/A
(B)
YFP-Spc110 C-toxic
Nud1-mTurquiose
Increased brightness
mCherry-Pus1
Merge
DIC
+ Gal
- Gal
N/A
YFP-Spc110 C-nontoxic
Nud1-mTurquiose
mCherry-Pus1
Merge
DIC
+ Gal
- Gal
(C)
YFP-Spc110 C-toxic
Nud1-mTurquiose
Tubulin-mCherry
Merge
DIC
+ Gal
- Gal
YFP-Spc110 C-nontoxic
Nud1-mTurquiose
Tubulin-mCherry
Merge
DIC
+ Gal
- Gal

We then asked whether overexpression of the Spc110 C-toxic fragment induces a cell cycle arrest. Analysis of DNA content by flow cytometry and budding index indicates that overexpression of the Spc110 C-toxic fragment causes cells to exhibit a G2/M cell cycle arrest as large-budded cells. In contrast, cells overexpressing the Spc110 C-nontoxic fragment proceed through the cell cycle normally (Supplemental Figure S2, B and C).

Overexpression of the Spc110 C-toxic fragment induces spindle irregularities and a defect in one SPB

To further understand the toxicity associated with overexpression of the Spc110 C-toxic fragment, we examined the localization of the SPBs in the arrested cells. Strikingly, when the Spc110 C-toxic fragment is overexpressed, one SPB appears to be located away from the nucleus as determined based on Hoechst staining of the DNA (Figure 2A, top panel). In contrast, in cells overexpressing the Spc110 C-nontoxic fragment, both SPBs exhibit normal localization associated with the DNA staining region (Figure 2A, bottom panel). We use the term "remnant" SPB to refer to the SPB that is located away from the nucleus because it is mislocalized compared with a wild-type SPB. We also found that the remnant SPB of the GFP-Spc110 C-toxic fragment consistently shows a 68% (±6%, n = 40) decrease in fluorescent signal from that of the other SPB. To further investigate whether the remnant SPB is detached from the nucleus, we used the nucleoplasmic marker Pus1-mCherry to visualize the nucleus (Smoyer *et al.*, 2016). Pus1 fills the entire nucleoplasm and can be used to analyze the shape of the nucleus (Friederichs *et al.*, 2011). In 95% (n = 40) of the cells overexpressing the Spc110 C-toxic fragment, the remnant SPB remains attached to nucleus by a string of nuclear membrane (Figure 2B, top panel). In contrast, in all cells overexpressing the Spc110 C-nontoxic fragment, the SPBs remain inside the nucleoplasm region (Figure 2B, bottom panel, n = 40). The remnant SPB of the YFP-Spc110 C-toxic fragment also showed a decrease in fluorescent intensity of 66% (±8%, n = 40) compared with the other SPB, consistent with the previous GFP fluorophore observation. Although both Spc110 C-toxic and Spc110 C-nontoxic form aggregates, the fluorescence intensity of the Spc110 C-toxic aggregate is 51% (±2%, n = 40) greater than the Spc110 C-nontoxic. We next examined the microtubules in cells overexpressing either the Spc110 C-toxic or the -nontoxic fragment to determine the effect on spindle organization and to gain a better understanding of the remnant SPB. Cells overexpressing Spc110 C-toxic fragment exhibited clearly disorganized microtubules with nonuniform signal along the spindle (Figure 2C, top panel). Defects include instances in which microtubules protrude from the aggregate and intersect with microtubules from the SPB, and other times only a small short microtubule stub is observed on the brightest SPB. The overexpression of the Spc110 homolog in the fission yeast *S. Pombe,* Pcp1p, also displayed microtubule abnormalities and arrays of microtubules nucleating from the non-SPB structures, similar to our observations (Flory *et al.*, 2002). Furthermore, the level of signal is higher for microtubules associated with the brighter SPB compared with the low level of microtubule signal associated with the remnant SPB. Nearly all of the cells overexpressing the Spc110 C-toxic fragment fail to assemble a bipolar spindle (> 96%, n = 30), whereas cells overexpressing the Spc110 C-nontoxic fragment exhibited normal bipolar spindles with uniform signal along the length of the spindle (Figure 2C, bottom panel).

We further analyzed the spindle defect phenotype using serial thin section electron microscopy (EM) and immuno-EM. Cells overexpressing the Spc110 C-toxic fragment, or the Spc110 C-nontoxic fragment, were induced with galactose for 3 h and the cells were then prepared for EM by high-pressure freezing and freeze-substitution (see *Materials and Methods*). Immuno-EM staining using anti-GFP antibodies and gold-labeled secondary fab fragments allowed us to determine the localization of the GFP-Spc110 C terminal fragments. Cells overexpressing the Spc110 C-nontoxic fragment displayed normal bipolar spindles as expected, along with the formation of the aggregate as observed by GFP fluorescence (Figure 3A). Consistent with live cell fluorescent imaging, the Spc110 C-nontoxic fragment localizes to the aggregate, but not to the SPBs. In contrast, cells overexpressing the Spc110 C-toxic fragment have defective spindles that emanate from a single SPB in large-budded cells, which would normally have a bipolar spindle (Figure 3B, n = 11 of 12 cells). Immuno-EM analysis using anti-GFP antibodies shows that the Spc110 C-toxic fragment localizes to both the aggregate and the SPBs, unlike the Spc110 C-nontoxic fragment. Our ability to detect monopolar spindles by EM in cells overexpressing the Spc110 C-toxic fragment was consistent with the results of our fluorescence microscopy imaging experiments; however, locating the remnant SPB in the cytoplasm was challenging when using EM. Despite this difficulty, we were able to observe what we believe is a remnant SPB in one of the imaged cells where the remnant is still in the vicinity of the nuclear envelope but appeared to lack structural integrity (Figure 3C, n = 1 of 12 cells, three serial-thin sections of the same cell are illustrated).

Overexpression of the Spc110 C-toxic fragment results in irreversible spindle defects in metaphase-arrested cells

Cells depleted of Cdc20, which is required for the metaphase-anaphase transition, arrest in metaphase with bipolar spindles (Zachariae and Nasmyth, 1999). When cells depleted of Cdc20 are arrested in

FIGURE 2: Overexpression of the Spc110 C terminus disrupts mitotic spindles. Fluorescence imaging of the Spc110 C-toxic and Spc110 C-nontoxic constructs after a 3-h incubation with 2% glucose (repressed) or 2% galactose (induced). An increased brightness panel for the green and yellow channel is shown in order to visualize the low GFP/YFP-Spc110 C-toxic signal associated with the remnant SPB. The remnant SPB is labeled with an R. (A) Shown are the Spc110 C-toxic (top panel) and Spc110 C-nontoxic (bottom panel). GFP-Spc110 C terminal fragment constructs (green; pMW2661, Spc110 AA741–944/Spc110 C-toxic; pMW2662, Spc110 AA741–923/Spc110 C-nontoxic), Nud1-Ruby2 (red), and DNA (blue). Remnant SPB showed a decrease in fluorescence intensity of 68% (±6%) compared with other SPB (n = 40). (B) Cells expressing the nuclear marker mCherry-Pus1 (red; pMW3274, pRS315-NOP1pr-GFP11-mCherry-Pus1), Nud1-mTurquiose (blue), Spc110 AA741–944/Spc110 C-toxic (yellow; pMW3195, top panel), and Spc110 AA741–923 (yellow; pMW3232, bottom panel). Spc110 C-toxic remnant SPB showed a decrease in fluorescence intensity of 66% (±8%, n = 40) compared with other SPB. Fluorescence intensity of Spc110 C-toxic aggregate is 51% (±2%, n = 40) greater than the Spc110 C-nontoxic aggregate. (C) Mitotic spindles from yeast cells showing microtubules (red), YFP-Spc110 C terminus construct Spc110 AA741–944/Spc110 C-toxic (yellow, top panel), Spc110 AA741–923/Spc110 C-nontoxic (yellow; bottom panel), and Nud1-mTurquioise (blue). Greater than 96% of the cells expressing the Spc110 AA741–944/Spc110 C-toxic fragment display disorganized spindles (n = 30). Bar, 2 μm. Arrowhead = SPB.

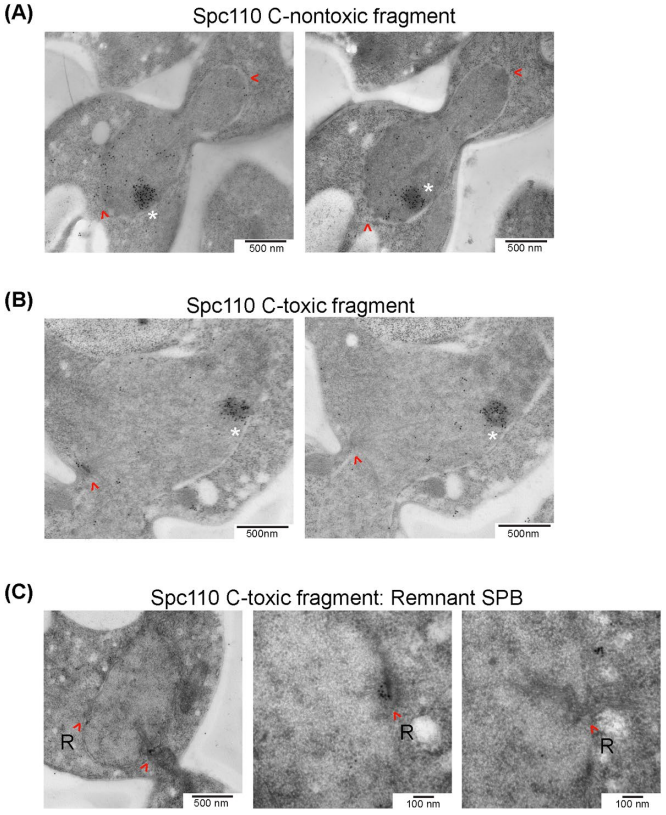

FIGURE 3: Overexpression of the Spc110 C terminus results in monopolar spindle and aggregate formation. Cell overexpressing either the GFP-tagged Spc110 C-toxic fragment (GFP-Spc110 AA741–944) or the GFP-tagged Spc110 C-nontoxic fragment (GFP-Spc110 AA741–923) were prepared for thin-section EM 3 h after galactose induction. (A) Cells overexpressing the Spc110 AA741–923/Spc110 C-nontoxic fragment had duplicated and separated SPBs and an aggregate, $N = 4$. (B) Eleven of 12 cells overexpressing the Spc110 AA741–944/Spc110 C-toxic fragment had one SPB and an aggregate. (C) In one out of 12 cells examined, a second SPB, which is a remnant SPB, can be observed. Red arrowhead, SPB; white asterisk, aggregate; and red arrow with R, remnant SPB.

metaphase, the SPBs grow 2.3-fold in size compared with wild-type cells, thus allowing the SPBs to nucleate an increased number of microtubules (O'Toole *et al.*, 1997). Since the SPBs are growing and increasing in their microtubule nucleation capacity, it can be inferred that SPB components can continue to be added to the SPB. We tested whether overexpression of the Spc110 C-toxic fragment had an effect on the ability of mature SPBs to nucleate microtubules. First, cells were arrested in metaphase without inducing the overexpression of the Spc110 C-toxic fragment by depleting Cdc20 using a methionine repressible promoter that turns off Cdc20 expression in the presence of methionine. Then the expression of the Spc110 C-toxic fragment was induced (+Gal) or not (–Gal) (Figure 4A). Short bipolar spindles and faint signal of the YFP Spc110 C-toxic fragment at the SPBs can be observed after Cdc20 depletion using methionine (Figure 4B). Surprisingly, overexpression of the Spc110 C-toxic fragment, even during a metaphase arrest, resulted in microtubule disorganization similar to that observed in cycling cells (Figure 4C). Cdc20-depleted cells are known to recover from the metaphase arrest and to progress through the cell cycle after the repression of Cdc20 is turned off (reviewed in Surana *et al.*, 2012). To test the effect of the overexpression construct on the reversibility of this arrest state, three different strains were plated on -MET plates to reverse the Cdc20 repression: normal cycling cells, Cdc20-depleted cells that were arrested, and Cdc20-depleted cells that were arrested and then induced to overexpress the Spc110 C-toxic fragment. The Cdc20-depleted cells that were arrested recovered and were similar to normal cycling cells after Cdc20 expression was restored, whereas the Cdc20 cells that were arrested and then induced to overexpress the Spc110 C-toxic fragment failed to recover from the arrest after Cdc20 expression was restored (Figure 4D). These results were surprising since experiments using fluorescence recovery after photobleaching (FRAP) have shown that during the assembly of the mitotic spindle, Spc110 is able to exchange in and out of the SPB until the spindle assembly is completed. After spindle assembly is complete, Spc110 is "stable" and Spc110 exchange is reduced (Yoder *et al.*, 2003; Viswanath *et al.*, 2017). Therefore, we expected the SPBs in Cdc20-depleted cells to not be affected by the overexpression of Spc110 C-toxic.

Overexpression of the Spc110 C-toxic fragment leads to a decrease in endogenous Spc110 at the remnant SPB

To investigate the behavior of endogenous Spc110 in cycling cells overexpressing either the Spc110 C-toxic or the Spc110 C-nontoxic construct, we used two different fluorescent labels to compare the localization of the overexpressed fragments (labeled with YFP) to that of full-length Spc110 (labeled with dsRed). Cells overexpressing the Spc110 C-nontoxic fragment showed a uniform distribution of endogenous full-length Spc110, with only a 5% (±2%) difference in the fluorescence intensity of full-length Spc110 between the two SPBs (Figure 5A, top panel, $n = 35$). In contrast, cells overexpressing the Spc110 C-toxic fragment showed an asymmetric distribution of endogenous Spc110 between the two SPBs, with a 69% (±4%) difference in the fluorescence intensity of full-length Spc110 between the two SPBs (Figure 5A, bottom panel, $n = 42$). We were able to discern by DNA staining that the SPB associated with the nucleus showed higher levels of endogenous Spc110 fluorescent signal, whereas the remnant SPB that is away from the nucleus showed lower levels of endogenous Spc110 fluorescent signal (Figure 5B, $n = 36$).

Our observation that overexpression of the Spc110 C-toxic fragment disrupted stable metaphase spindles in Cdc20-depleted cells was an unexpected result. Therefore, we were particularly interested in examining the distribution of endogenous full-length Spc110 at the SPBs in cells arrested by Cdc20 depletion that were overexpressing the toxic Spc110 C terminal fragment. We imaged the localization of endogenous Spc110-dsRed in Cdc20-depleted cells in the absence (Figure 5C, top panels) or presence of galactose to induce the expression of the Spc110 C-toxic fragment (Figure 5C, bottom panels). In this context, we also observed an unequal distribution of endogenous Spc110 between the two SPBs, with a 29% (±2%, $n = 30$) difference in the fluorescence intensity of full-length Spc110 between the two SPBs, after the induction of the Spc110 C-toxic fragment in the Cdc20-depleted cells. A 39% (±5%, $n = 30$) difference in the YFP fluorescence intensity of Spc110 C-toxic fragment was also observed between the two SPBs. DNA staining revealed that the SPB with the decreased amount of endogenous Spc110 is located away from the nucleus (Supplemental Figure S3). This suggests that diminished endogenous Spc110 at the remnant SPB may be contributing to the toxic phenotype.

Spc110 binding to Spc42 and Spc29

Spc110 has been shown to bind to the central plaque proteins Spc42 and Spc29 via its C terminus (Adams and Kilmartin, 1999;

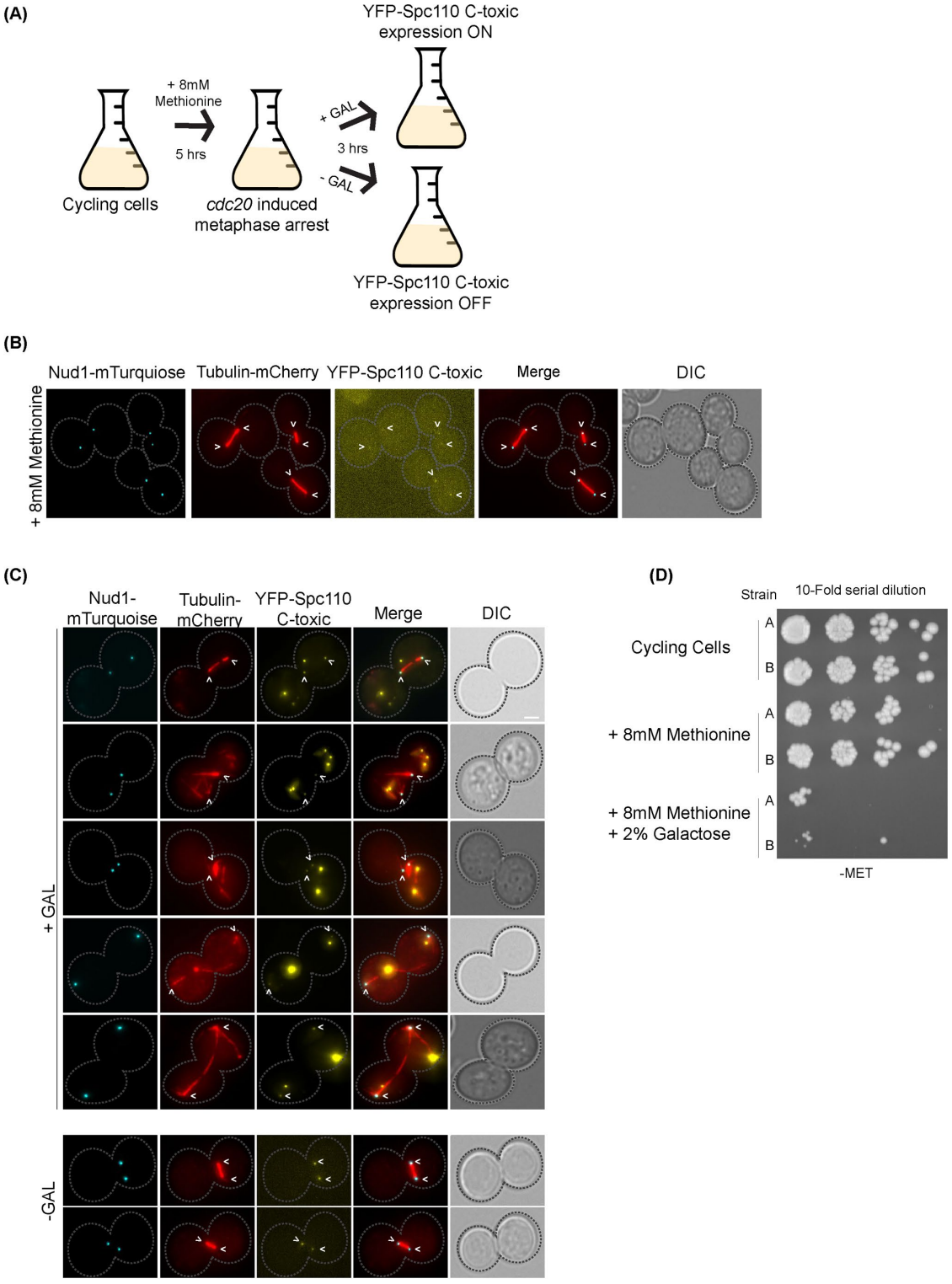

FIGURE 4: Cells overexpressing the toxic Spc110 AA741–944 C terminal fragment fail to recover from a G2/M arrest following Cdc20 depletion. (A) Flow chart diagram of the cdc20 depletion assay. (B) Cells expressing Cdc20 under the control of a methionine repressible promoter were incubated in YEP + 2% raffinose with 8 mM methionine for 5 h at 30°C. Shown are Nud1-mTurquioise (blue), microtubules (red), and the toxic Spc110 AA741–944 C terminal fragment (yellow; Spc110 C-toxic). (C) Cells from A were incubated either in the presence ($n = 55$) or in the absence of 2% galactose ($n = 37$). (D) Tenfold serial dilution of the cells from B and from cells that received no treatment (cycling cells) were spotted onto -Met plates and grown for 2 d at 30°C. Bar, 2 µm. Arrowhead, SPB.

Elliott *et al.*, 1999). To determine which amino acid residues are required for Spc110 binding to these two central plaque proteins and how this relates to the toxicity of Spc110 C-toxic fragment expression, we introduced the truncation series shown in Figure 1B into a yeast two-hybrid system and monitored the interactions. It was previously shown that the C terminal 163 amino acid residues of Spc110

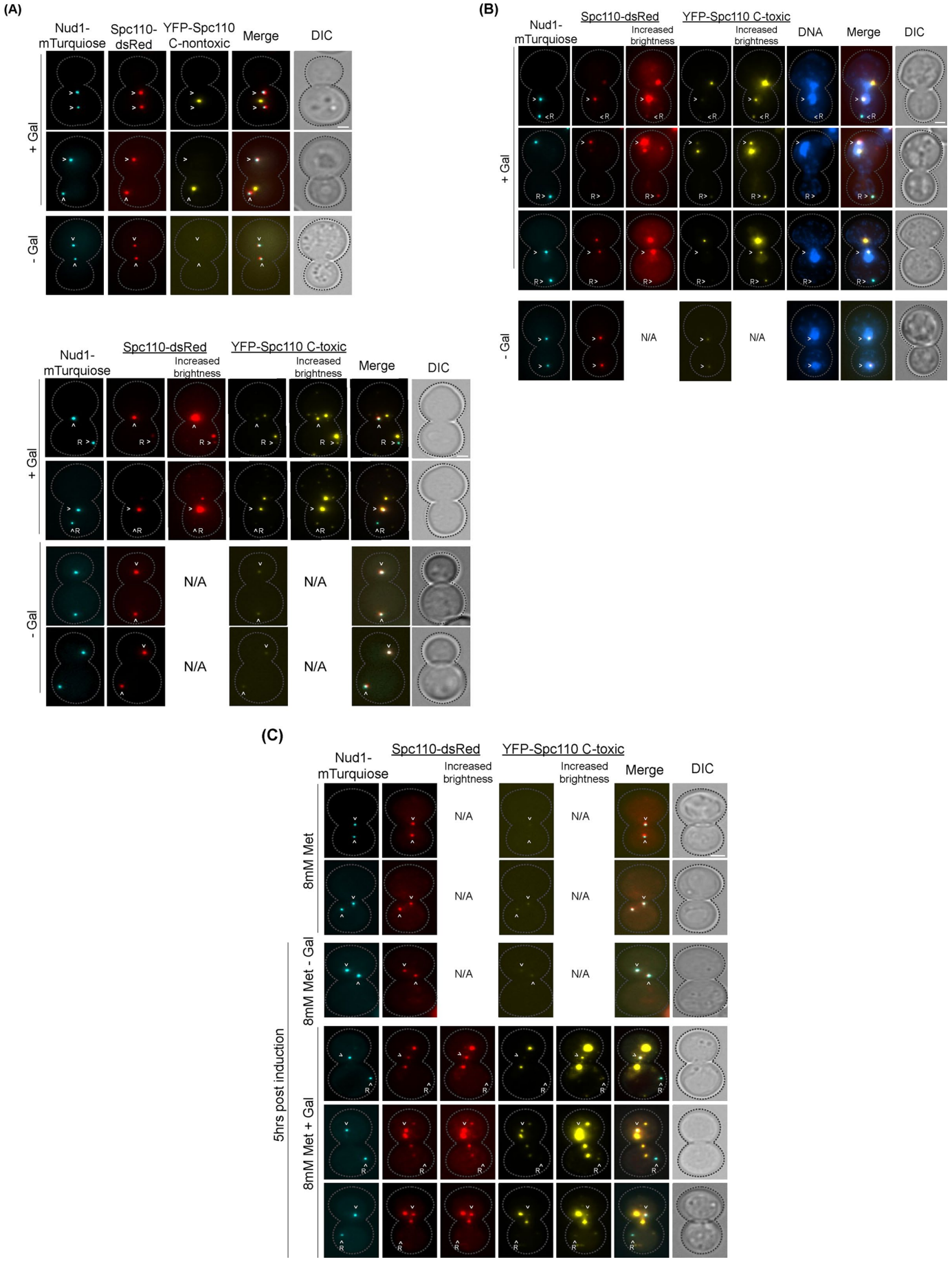
(A)
Nud1-mTurquiose
Spc110-dsRed
YFP-Spc110 C-nontoxic
Merge
DIC
+ Gal
- Gal
Nud1-mTurquiose
Spc110-dsRed
Increased brightness
YFP-Spc110 C-toxic
Increased brightness
Merge
DIC
+ Gal
- Gal
N/A
N/A
N/A
N/A
(B)
Nud1-mTurquiose
Spc110-dsRed
Increased brightness
YFP-Spc110 C-toxic
Increased brightness
DNA
Merge
DIC
+ Gal
- Gal
N/A
N/A
(C)
Nud1-mTurquiose
Spc110-dsRed
Increased brightness
YFP-Spc110 C-toxic
Increased brightness
Merge
DIC
5hrs post induction
8mM Met
8mM Met - Gal
8mM Met + Gal
N/A
N/A
N/A
N/A
N/A
N/A

are required for binding to the N terminus of Spc42 (Kilmartin and Goh, 1996); here, we show that interaction of the Spc110 C terminus with full-length Spc42 is greatly diminished when only the C terminal 21 amino acid residues of Spc110 are deleted (Figure 6A, see AD-Spc110-741–923 vs. AD-Spc110-741–944). Taken together with our observation that the Spc110 C-nontoxic fragment, which includes Spc110 C terminal residues 741–923, fails to be recruited to the SPB suggests that Spc42 binding to Spc110 is a key determinant in this process. Spc29 binding to Spc110 had previously been mapped to Spc110 C terminal residues 800–898 (Elliott *et al*., 1999). Here, we demonstrate that the highly conserved amino acid residues 799–856 in Spc110 are sufficient for binding to Spc29 (Figure 6B) (Lin *et al*., 2014; Viswanath *et al*., 2017). A Bayesian integrative modeling approach has previously been used to model the structure of the SPB, including Spc110 binding to the SPB (Viswanath *et al*., 2017). This model predicted that Spc110 binding to the SPB occurs via two redundant binding regions, including residues 783–811 and 812–838. These two regions are thought to be in close proximity to Spc42 and possibly to Spc29. Consistent with this model, our experiments using yeast two-hybrid analysis show that Spc42 does not bind to the C terminus of Spc110 when residues 783–838 are deleted (Figure 6C, left panel), but that Spc29 is still able to bind (Figure 6C, middle panel). The localization of fluorescently labeled Spc42 and Spc29 to the SPB was also tested in the strains overexpressing the Spc110 C-toxic or the Spc110 C-nontoxic fragment. Although Spc42 and Spc29 localized to the SPBs in cells overexpressing either the Spc110 C-toxic or the Spc110 C-nontoxic fragment, Spc42 and Spc29 are disproportionately distributed between the two SPBs in the Spc110 C-toxic cells. There is a difference in fluorescence intensity of 44% (±3%) for Spc42 and 46% (±2%) for Spc29 between the two SPBs in the Spc110 C-toxic construct compared with 22% (±1%) for Spc42 and 19% (±4%) for Spc29 in the Spc110 C-nontoxic construct. Also, more Spc42 (56% ± 2%) and Spc29 (72% ± 4%) localize to the aggregate in the cells overexpressing the Spc110 C-toxic fragment (Figure 6, D and E, $n = 46$ and $n = 40$, respectively). The increased signal for Spc42 is consistent with the observation that the Spc110 C-toxic fragment contains a domain, including residues 923–944, that facilitates Spc42 binding. It is likely that the increased localization of Spc29 in the SPB aggregate is due to its interaction with Spc42.

Role of Spc110 and Cmd1 in SPB assembly

We were interested in examining the role of Cmd1 with regard to the toxicity of the Spc110 C-toxic fragment and its localization to the SPB. Cmd1 has been shown to bind to the Spc110 C terminus between residues 900–913 (Geiser *et al*., 1991, 1993; Stirling *et al*., 1994, 1996) and to strengthen the SPB-microtubule attachment (Fong *et al*., 2017). A double point mutation in the Cmd1-binding domain of Spc110 (V908E and R913W, *spc110-111*) inhibits Cmd1 binding and leads to cell death when the mutant allele is present in a single copy in the genome (Stirling *et al*., 1994). Strains with additional copies of the mutant allele are viable but temperature sensitive (Stirling *et al*. 1994). Overexpression of the Spc110 C-toxic fragment harboring the V908E and R913W mutations (Spc110 C-toxic-V908E R913W) was not toxic at either the permissive or the restrictive temperature (Figure 7A, row 3, SI). However, we found that this mutant version of the Spc110 C-toxic fragment was expressed at a lower level than the original Spc110 C-toxic fragment (Supplemental Figure S4, lane 6, single insert SI vs. lane 5), which is likely to affect its toxicity. Therefore, we integrated multiple copies of the GAL1-Spc110 Spc110 C-toxic-V908E R913W allele to achieve higher expression levels compared with that of the Spc110 C-toxic fragment lacking the point mutations (Supplemental Figure S4, lane 7 multiple inserts [MI] vs. lane 5). Overexpression of this Cmd1-binding mutant construct (called MI) was toxic at the permissive temperature, but not at the restrictive temperature (Figure 7A, row 4), despite being expressed at a level equal to or higher than the original Spc110 C-toxic fragment at 37˚C (Supplemental Figure S4, lane 10 vs. lane 8). Correspondingly, the Spc110 C-toxic-V908E R913W mutant allele localized to the SPB at the permissive temperature (Figure 7B, top panel), and very little was observed at the SPB at the restrictive temperature (Figure 7B, bottom panel). These results strikingly parallel the behavior of the *spc110-111* mutant allele in the endogenous gene and suggest that binding to Cmd1 is essential both for the toxicity of the Spc110 C-toxic fragment and for Spc110 localization to the SPB.

DISCUSSION

A toxic domain of Spc110

Found on the nuclear face of the SPB, the essential component Spc110 is organized into three domains. The globular N terminal domain of Spc110 binds to the γ-tubulin complex and aids in the nucleation of microtubules (Knop and Schiebel, 1997; Nguyen *et al*., 1998). The central domain of Spc110, an extended coiled-coil required for dimer formation, acts as a spacer between the central plaque and the inner plaque of the SPB (Kilmartin and Goh, 1996; Muller *et al*., 2005; Viswanath *et al*., 2017). The presumed globular C terminus of Spc110, which is localized to the central plaque, anchors Spc110 dimers to the SPB via interactions with other SPB components, including Spc42, Spc29, and Cmd1 (Geiser *et al*., 1993; Stirling and Stark, 2000). Here, we investigated the domains required for the localization of the Spc110 C terminus to the SPB.

FIGURE 5: Overexpression of the toxic Spc110 AA741–944 C terminal fragment results in asymmetric distribution of endogenous Spc110 between the two SPBs. Fluorescence quantification of endogenous Spc110 signal after 3-h induction of the overexpression of the Spc110 C-toxic fragment or Spc110 C-nontoxic fragment in galactose or repression in glucose. Increased brightness panels for the red and yellow channels are shown in order to visualize the very low endogenous levels of Spc110-dsRed and YFP Spc110 AA741–944/Spc110 C-toxic fragment signal associated with the remnant SPB. The remnant SPB is labeled with an R. (A) Nud1-mTurquioise (blue), endogenous Spc110-dsRed (red), YFP-Spc110 C terminal fragment constructs (yellow): pMW3232, Spc110 AA741–923/Spc110 C-nontoxic, 5% (±2%) difference in the fluorescence intensity of full-length Spc110 between the two SPBs (top panel, $n = 35$); pMW3195, Spc110 AA741–944/Spc110 C-toxic, 69% (±4%) difference in the fluorescence intensity of full-length Spc110 between the two SPBs (bottom panel, $n = 42$). (B) DNA staining of cells overexpressing the Spc110 C-toxic fragment ($n = 36$). (C) Cells were arrested in G2/M via the repression of *Cdc20* expression with 8 mM methionine for 5 h at 30°C. The cells were then incubated with or without 2% galactose. 29% (±2%, $n = 30$) of endogenous Spc110 was unequally distributed between the two SPBs after Spc110 C-toxic induction. There was also a 39% (±5%, $n = 30$) difference in YFP fluorescence intensity between the two SPBs. Bar, 2 μm. Arrowhead, SPB.

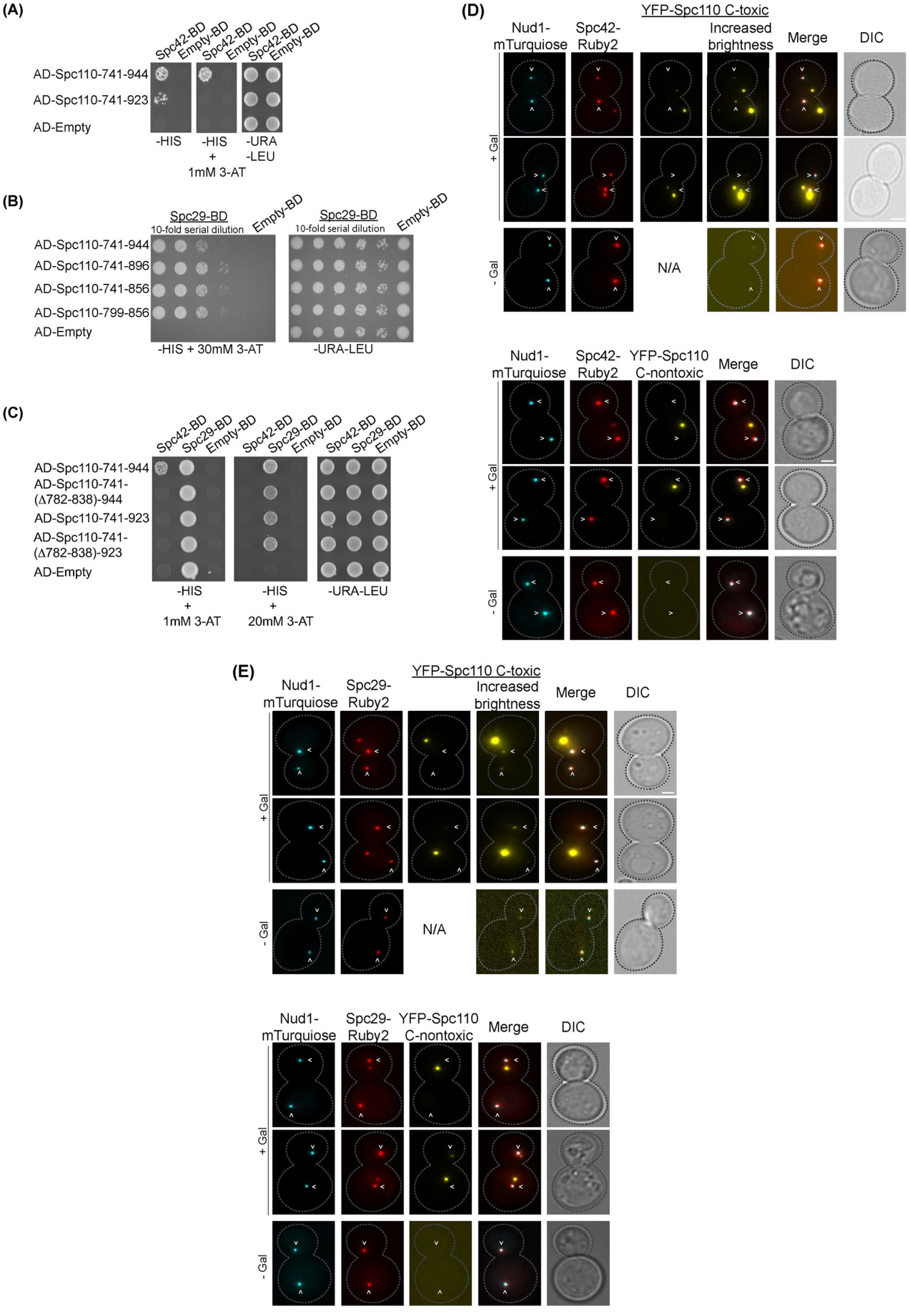
(A)
Spc42-BD
Empty-BD
Spc42-BD
Empty-BD
Spc42-BD
Empty-BD
AD-Spc110-741-944
AD-Spc110-741-923
AD-Empty
-HIS
-HIS + 1mM 3-AT
-URA -LEU
(B)
Spc29-BD
10-fold serial dilution
Empty-BD
Spc29-BD
10-fold serial dilution
Empty-BD
AD-Spc110-741-944
AD-Spc110-741-896
AD-Spc110-741-856
AD-Spc110-799-856
AD-Empty
-HIS + 30mM 3-AT
-URA-LEU
(C)
Spc42-BD
Spc29-BD
Empty-BD
Spc42-BD
Spc29-BD
Empty-BD
Spc42-BD
Spc29-BD
Empty-BD
AD-Spc110-741-944
AD-Spc110-741-(Δ782-838)-944
AD-Spc110-741-923
AD-Spc110-741-(Δ782-838)-923
AD-Empty
-HIS + 1mM 3-AT
-HIS + 20mM 3-AT
-URA-LEU
(D)
YFP-Spc110 C-toxic
Nud1-mTurquiose
Spc42-Ruby2
Increased brightness
Merge
DIC
+ Gal
- Gal
N/A
Nud1-mTurquiose
Spc42-Ruby2
YFP-Spc110 C-nontoxic
Merge
DIC
+ Gal
- Gal
(E)
YFP-Spc110 C-toxic
Nud1-mTurquiose
Spc29-Ruby2
Increased brightness
Merge
DIC
+ Gal
- Gal
N/A
Nud1-mTurquiose
Spc29-Ruby2
YFP-Spc110 C-nontoxic
Merge
DIC
+ Gal
- Gal

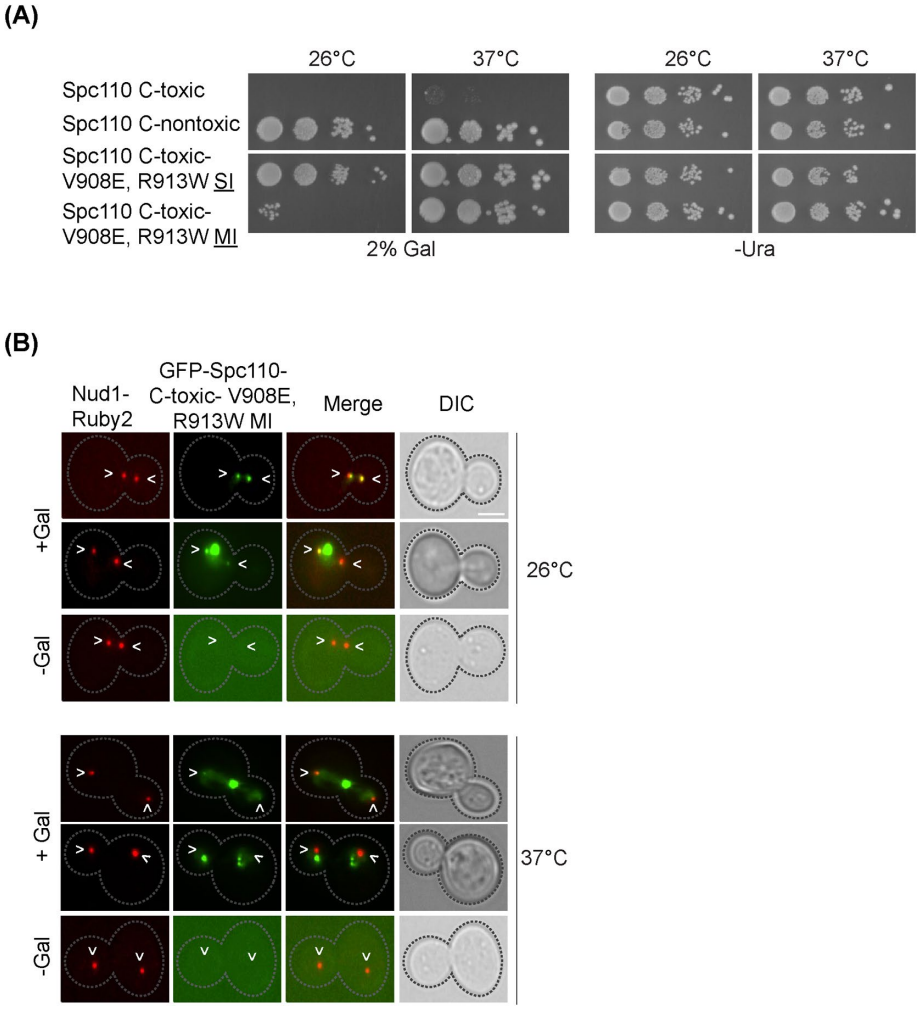

FIGURE 7: The Spc110 Cmd1-binding domain is necessary for its localization to SPBs. (A) Fivefold serial dilutions of strains expressing Spc110 AA741–944/Spc110 C-toxic (pMW2661), Spc110 AA741–923/Spc110 C-nontoxic (pMW2662), Spc110 AA741-V908E, R913W-944 single/multi-insert (pMW3140) were spotted onto 2% galactose and -URA plates. Plates were incubated at 26 or 37°C for 2 d. Images are from the same plate; a row was cropped out of the image. (B) Representative fluorescent images of strains expressing the single/multi-GFP-Spc110 AA741-V908E, R913W-944 (green) construct at 26° and 37°C are shown together with Nud1-Ruby2 (red) localization. Bar, 2 μm. Arrowhead, SPB.

We explored the overexpression phenotype to determine whether the aggregate formation or the mechanism associated with its toxicity could provide new insights about SPB biology and to determine whether it may serve as the basis for an assay to identify additional binding domains within the Spc110 C terminus. We show that the aggregate formed by overexpression of the Spc110 C terminal nucleates microtubules and sequesters a number of SPB components, including Spc42, Spc29, and Spc110. While binding of the SPB components to the aggregate may affect SPB structure and function via titration of SPB components, the fact that the Spc110 C-nontoxic construct also forms a nuclear aggregate that contains SPB components, but does not nucleate microtubules or result in SPB or growth phenotypes, suggests that the aggregates themselves do not contribute significantly to the SPB and growth phenotypes we observed.

Overexpression of the Spc110 C-toxic fragment causes mitotic spindle defects that lead to a G2/M cell cycle arrest (discussed below, Figure 8). During metaphase, the SBPs are stable and Spc110 molecules are presumed to be equally distributed between the two SPBs. Uniform distribution of Spc110 helps recruit the appropriate number of γ-tubulin complexes to the SPB for proper microtubule nucleation to occur. Once the Spc110 C-toxic fragment is turned on, endogenous Spc110 is displaced from one SPB which gives rise to a remnant SPB. This remnant SPB contains the Spc110 C-toxic fragment, which lacks γ-tubulin complex-binding domain and therefore lacks the ability to nucleate microtubules. Beside endogenous Spc110 being displaced from one SPB, aggregates start to form which sequester a number of SPB components, including Spc29, Spc42, and endogenous Spc110. Without the proper number of microtubules nucleating from one of the two SPBs to balance out the spindle forces the spindle is unstable and the remnant SPB is pulled away from the nucleus causing microtubule disorganization, which suggests full-length Spc110 is required to maintain SPB integrity. This is similar to defects associated with other *spc110* mutations

Our initial experiment investigating the function of the Spc110 C terminus was designed to test whether it localized to SPBs as an isolated domain. Perhaps the Spc110 C terminal domain localizes to the SPB when overexpressed, but we unexpectedly found that the overexpressed domain formed aggregates in the nucleoplasm in addition to localizing to the SPB, and that it was toxic to yeast cells.

FIGURE 6: Identification of domains within the Spc110 C terminus that are necessary for interacting with Spc42 and Spc29. (A–C) Yeast two-hybrid interactions of AD-Spc110 741–944/Spc110 C-toxic, AD-Spc110 741–923/Spc110 C-nontoxic, AD-Spc110 741–896, AD-Spc110 741-856, AD-Spc110 799–856, AD-Spc110 741-(Δ782-838)-944, and AD-Spc110 741-(Δ782-838)-923, with Spc42-BD (A, C) and Spc29-BD (B, C) are shown. Cells were selected on medium lacking uracil and leucine (-URA –LEU) and assayed for interactions on medium lacking histidine (-HIS), -HIS + 1 mM 3-AT, or -HIS + 30 mM 3-AT. Growth was scored after incubation at 30°C for 2-3 d. (D) Fluorescent localization of Spc42 with the toxic and nontoxic Spc110 C terminal fragments. Nud1-mTurquioise (blue), Spc42-Ruby2 (red), and YFP-Spc110 C terminal fragment construct (yellow; pMW3195, Spc110 AA741–944/Spc110 C-toxic; pMW3232, Spc110 AA741–923/Spc110 C-nontoxic). **(E)** Localization of Spc29 with the toxic and nontoxic Spc110 C terminal fragments. Nud1-mTurquioise (blue), Spc29-Ruby2 (red), and YFP-Spc110 C terminus construct (yellow; pMW3195, Spc110 AA741–944/Spc110 C-toxic; pMW3232, Spc110 AA741–923/Spc110 C-nontoxic). Bar, 2 μm. Arrowhead, SPB.

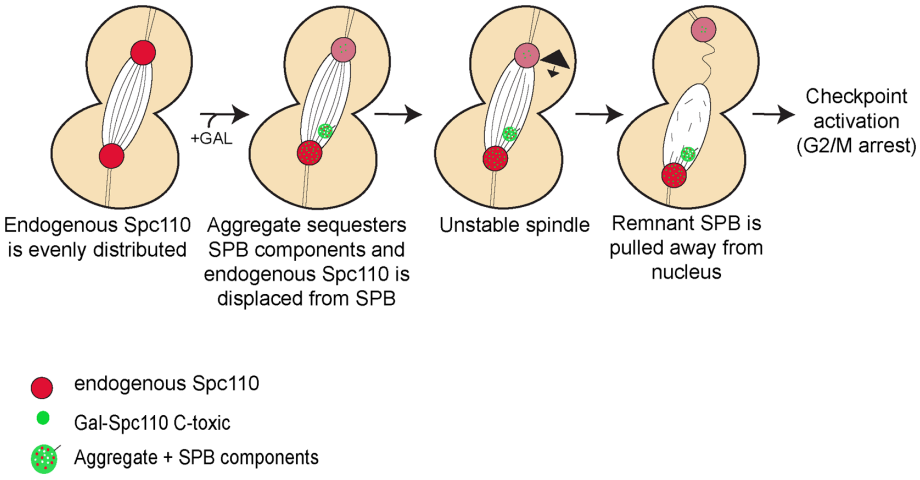

FIGURE 8: Model showing how the overexpression of the toxic Spc110 C terminal fragment induces cell cycle checkpoint activation. See text for details.

(i.e., *spc110–226*; Yoder *et al.*, 2005). Thus, we propose the defective SPBs are largely responsible for the observed phenotypes. Interestingly, overexpression of Spc110 1-Δ216–600-944 was shown previously to be similarly toxic and to give rise to spheroidal polymers that accumulated in the nucleus (Kilmartin and Goh, 1996). It is possible that this construct, similar to the Spc110 C-toxic fragment, is able to localize to the SPB and displace wild-type Spc110, but is lacking an essential function and is therefore toxic to the cell. Our data indicate that the toxicity associated with Spc110 overexpression is due to the C terminal domain and is not associated with the Spc110 N terminus. In addition, overexpression of full-length Spc110 was not toxic, presumably because it can function when it localizes to the SPB.

An extraordinary feature of the Spc110 C-toxic fragment is its ability to induce the formation of the remnant SPB. As noted above, the appearance of remnant SPBs suggests that the inclusion of full-length Spc110 into the SPB is required for the stability of the structure in some way that cannot be duplicated by the C terminal domain. The SPB structure model (Viswanath *et al.*, 2017) suggests that interactions of core SPB components with Spc110 occur outside of the domain we tested and that perhaps these interactions are important for SPB stability. It is also interesting that both the formation and the segregation of the remnant SPB are asymmetric. In cycling cells, it is easy to see that the remnant SPB could arise from an inability to form a new SPB during mitosis in the presence of the overexpressed Spc110 C terminus, similar to mutants that block SPB assembly or generate defective SPBs (i.e., *mps2-1*, *ndc1-1*, *bbp1-1* mutants; Winey *et al.*, 1991, 1993; Schramm *et al.*, 2000; Lau *et al.*, 2004). The newly synthesized SPB could be defective and unable to withstand the cytoplasmic microtubule forces exerted to keep the spindle positioned for proper SPB segregation to occur. In fact, it is difficult to discern from our data whether the old or the new SPB becomes the remnant. At first glance, our experiments suggest the alternative, that is, that the remnant SPB arises from the old SPB since it is localized to the daughter cell bud 84% of the time, which is the normal inheritance observed for the old SPB (Winey and O'Toole, 2001). However, the overexpression of the Spc110 C-toxic fragment results in substantial microtubule defects, which could also affect typical patterns of SPB segregation. Also, we tested cells arrested in metaphase using Cdc20 depletion and found that overexpression of the Spc110 C-toxic fragment can result in damage to fully assembled, intact SPBs. This finding suggests that components can be incorporated into SPBs during mitosis despite a FRAP study showing little turnover (Yoder *et al.*, 2003). In addition, while we may not understand all of the pathology associated with overexpression of the C terminus of Spc110, our work suggests a potential paradigm for a class of centrosome defects.

Domains necessary for recruitment of the Spc110 C terminus to the SPB

The structure-function analysis that we undertook was to determine the domains within the Spc110 C terminus responsible for its localization to the SPB. The most surprising result was that the removal of the C terminal 21 residues of the Spc110 C terminus renders it unable to localize to the SPB and nontoxic when overexpressed. Our yeast two-hybrid data indicate that the C terminal 21 residues of Spc110 play a role in the binding of Spc110 to Spc42. We propose that the loss of this interaction prevents the Spc110 C-nontoxic fragment from localizing to the SPB, which in turn prevents the toxic phenotype. Interestingly, an integrated *SPC110* gene that lacks the C terminal 21 amino acids is viable, but the spores do appear to be smaller in size compared with the full length *SPC110* control (Supplemental Figure S5). A gene carrying *SPC110 AA1-927* had previously also been shown to complement an *SPC110* null strain (Geiser *et al.*, 1993). Thus, the C terminal 21 amino acids are important, but not essential for full-length Spc110 to interact with Spc42. Indeed, our yeast two-hybrid data revealed a second Spc42 binding site on Spc110, since a decrease in the Spc42-Spc110 protein interaction was also observed when residues 782-838 were deleted from the Spc110 C terminus. This data is consistent with the Spc42-Spc110 binding site predicted based on the SPB structure model, in which region N782-Y838 of Spc110 is predicted to be exposed to a layer of Spc42 in the central plaque (Viswanath *et al.*, 2017).

Our two-hybrid data also narrows down the Spc29 binding region on Spc110, which was previously shown to include S800-A898 (Elliott *et al.*, 1999), to residues D799-I856. Notably, this region of Spc110 is highly conserved across different types of yeast. The SPB structure model from Viswanath *et al.* (2017) predicted a possible binding site for Spc29 between residues N782-Y838. In our two-hybrid assay, Spc29 interacted with Spc110 when N782-Y838 was deleted, but it is possible that there is an additional binding site for Spc29 within the Spc110 C terminus.

Previous research has shown that Cmd1 binding to Spc110 is necessary for Cmd1 localization to the SPB and for strengthening SPB-microtubule attachment, as tested by direct force measurements on isolated SPBs (Geiser *et al.*, 1993; Fong *et al.*, 2017). It is thought that Cmd1 helps crosslink nearby Spc110-Cmd1 complexes, thereby stabilizing the central plaque (Viswanath *et al.*, 2017). Here, we inhibited Cmd1 binding by introducing two known temperature-sensitive point mutations, V908E and R913W, into the Cmd1-binding domain of the Spc110 C-toxic fragment, (Stirling *et al.*, 1994). The Spc110 V908E R913W C terminal fragment mutant protein failed to localize to the SPB at the nonpermissive temperature. These mutations also relieve the toxic phenotype associated with the overexpression of the Spc110 C-toxic fragment, which is consistent with the Spc110 C terminus not being recruited to the

Strains	Genotype	Source or reference
yMW4386	*MATa cdc20Δ::MET3p-CDC20-KanMX*	M. Gartenberg
yMW4908	*MATa* Spc110-dsRed::KanMX	J. Moore
yMW5226	*MATa/MATα* SPC110/spc110Δ::KanMX	This study
yMW5227	*MATα* Trp1-901 leu2-112 ura3-52 his3-200 gal4Δ gal80Δ LYS2-::GAL1-His3 Gal2-ADE2 met2::GAL7-lacZ	(James *et al.*, 1996)
yMW5404	*MATa Spc29-yomRuby2::KanMX*	This study
yMW5412	*MATa Nud1-yomRuby2::spHis5*	This study
yMW5414	*MATa Spc72-yomRuby2::spHis5*	This study
yMW5471	*MATα* Nud1-mTurquoise2::SpHis5	This study
yMW5908	*MATa Spc42-yomRuby2::KanMX Ade2+*	This study
yMW5967	*MATa* Spc110-yomRuby2::Hygro	This study

TABLE 1: Strains used in this study.

SPB. Together, these findings suggest that the Spc29 binding domain, the Cmd1-binding domain, and the Spc42 binding regions are all necessary for Spc110 recruitment to the SPB.

Lessons for pericentrin

Chromosome instability is a common feature of many human cancers due to chromosome missegregation during mitosis (Lengauer *et al.*, 1998; Pihan *et al.*, 1998). Increased levels of pericentrin in higher organisms have been shown to cause centrosome defects, abnormal spindles, and chromosome instability that may lead to cancer [reviewed in ((Delaval and Doxsey, 2010)]. A transgenic mouse model with increased pericentrin levels shows features of carcinoma (Delaval and Doxsey, 2010). In addition, expression of pericentrin in human prostate cells resulted in abnormal spindles and chromosome instability (Delaval and Doxsey, 2010). Pericentrin is a centrosome scaffold protein that can bind several proteins, including the γ-tubulin complex, which nucleates microtubules, and Cmd1. These interactions are conserved and important for its function from yeast to human, in which Spc110 is the homolog of pericentrin. Therefore, common features of Spc110 may be preserved in higher organisms. Here, we show that the overexpression of Spc110 C terminus leads to defective centrosomes in yeast together with extensive microtubule defects. These abnormalities could lead to chromosome instability in higher organisms and give us insights into mechanisms of tumorigenesis.

MATERIALS AND METHODS

Plasmid construction

The Rayment lab at the University of Wisconsin-Madison generated a series of deletion constructs corresponding to the Spc110 C terminus. Site-directed mutagenesis and domain deletions were performed using the QuikChange II mutagenesis kit (Stratagene) using pMW2661 as the parent backbone. All of the constructs were sequence-verified.

Yeast strains

Yeast strains used in this study are all derived from the W303 background and are listed in Table 1. Fluorescent protein tags, including mTurquioise2, Ruby2, and mCherry, were generated via PCR gene tagging in yMW1522 or yMW698 (Longtine *et al.*, 1998; Gardner and Jaspersen, 2014). The various plasmids harboring Spc110 C terminal fragments are listed in Table 2 and were linearized with ApaI and integrated into a yMW1522 or yMW698 yeast strain at the *URA3* locus.

Toxicity plate assay

Strains containing the various constructs were grown to an OD600 of 0.4 in YEP media containing 2% raffinose. Tenfold serial dilutions were spotted onto plates containing either glucose (repressing) or 2% galactose (inducing). Plates were incubated for 2–3 d at 30°C prior to imaging.

Cell cycle profiling

The stage of the cell cycle was determined using the Muse Cell analyzer instrument in conjunction with the Muse cell cycle assay kit (Millipore Sigma) according to manufacturer's instructions.

Complementation assay

A Spc110 AA1-944-Trp+ and Spc110 AA1-923-Trp+ construct was integrated into the TRP locus of a diploid Spc110 null strain. Diploids were sporulated, and the tetrads were dissected on YPD plates. Spores were analyzed for viability after 4 d at 30°C. YPD plate were then replica plated onto a -TRP plate and imaged the following day.

Fluorescence microscopy

Localization experiments were conducted by growing strains to log-phase in medium containing 2% raffinose at 30°C. Two percent galactose was then added, and the cells were shaken at 30°C for 3 h. Cells were then fixed with 4% formaldehyde in 100 mM sucrose for 15 min at room temperature, pelleted, and washed twice with phosphate-buffered saline (PBS) (pH 7.4). Images were acquired on an inverted microscope Eclipse Ti-E (Nikon) fitted with a CFI60 Plan Apochromat lambda 100× oil immersion objective lens (N.A. 1.45) (Nikon) and an ORCA-Flash4.0 V3 sCMOS camera. Hoechst DNA dye was imaged using a 350/50 nm excitation and 460/50 nm emission filter. mTurquoise was imaged using a 436/20 nm excitation and ET480/40 nm emission filter. YFP was imaged using a 500/20 nm excitation and ET535/30 nm emission filter. GFP was imaged using a 470/40 nm excitation and ET525/50 nm emission filter. mCherry and Ruby2 were imaged using a 560/40 nm excitation and ET630/70 emission filter. Data were acquired using NIS-Elements software. Image projections were made in ImageJ software (National Institutes of Health [NIH]).

Fluorescence intensity quantification. For fluorescence intensity quantification, a z-stack of 21 sections at a 0.2-μm step was taken. The z-stack was maximum projected, and the integrated intensity was acquired using an 8 × 8-pixel square around the SPB. The

Plasmids	Genotype	Source or reference
pMW2661	pRS306-Gal-NLS-GFP-Gp7-Spc110 (741–944) Amp^R	This study
pMW2662	pRS306-Gal-NLS-GFP-Gp7-Spc110 (741–923) Amp^R	This study
pMW2663	pRS306-Gal-NLS-GFP-Gp7-Spc110 (741–896) Amp^R	This study
pMW2666	pRS306-Gal-NLS-GFP-Gp7-Spc110 (741–813) Amp^R	This study
pMW2668	pRS306-Gal-NLS-GFP-Gp7-Spc110 (741-(Δ799–878)-944) Amp^R	This study
pMW2669	pRS306-Gal-NLS-GFP-Gp7-Spc110 (741-(Δ799–917)-944) Amp^R	This study
pMW2670	pRS306-Gal-NLS-GFP-Gp7-Spc110 (799–856) Amp^R	This study
pMW2687	pRS306-Gal-NLS-GFP-Gp7-Spc110 (799–856) Amp^R	This study
pMW2898	pRS304_KanMX -Spc110 1-944 Amp^R	This study
pMW2964	pGBDU-C1 Spc29 Amp^R	This study
pMW2965	pGAD-C1 Spc110-(741-856) Amp^R	This study
pMW2966	pGAD-C1 Spc110-(799–856) Amp^R	This study
pMW2967	pGAD-C1 Spc110-(741–944)Amp^R	This study
pMW2968	pGAD-C1 Spc110-(741–896) Amp^R	This study
pMW2979	pGAD-C1 Spc110-(741–923)Amp^R	This study
pMW2981	pGBDU-C1 Spc42 Amp^R	This study
pMW2982	pGAD-C1 Spc110-(1-944) Amp^R	This study
pMW3029	pRS304_KanMX-Spc110 1-923 Amp^R	This study
pMW3049	pRS306-Gal-NLS-GFP-Gp7-Spc110 (813–944) Amp^R	This study
pMW3053	pRS306-Gal-NLS-GFP-Gp7-Spc110 (896–944) Amp^R	This study
pMW3099	pRS305-Tub1-mCherry Amp^R	This study
pMW3136	pGAD-C1 Spc110 (741-V908E,R913W-944) Amp^R	This study
pMW3138	pGBDU-C1-Spc110 (741-V908E,R913W-944) Amp^R	This study
pMW3140	pRS306-Gal-NLS-GFP-Gp7-Spc110 (741-V908E,R913W-944) Amp^R	This study
pMW3195	pRS306-YFP-Gal-NLS-Gp7-Spc110 (741–944) Amp^R	This study
pMW3232	pRS306-Gal-NLS-YFP-Gp7-Spc110 (741–923) Amp^R	This study
pMW3250	pGAD-C1 Spc110-AA741-(Δ782-838)-923 Amp^R	This study
pMW3267	pGAD-C1 Spc110-AA741-(Δ782-838)-944 Amp^R	This study
pMW3274	pRS315-NOP1pr-GFP11-mCherry-Pus1 Leu2+ Amp^R	S. Jaspersen

TABLE 2: Plasmids used in this study.

percentage difference between the two SPBs was calculated using the following equation: %difference = |100 × (intensity 1 – intensity 2)/intensity 1|. The same method was performed to calculate the difference in fluorescence intensity of the aggregate in the Spc110 C-toxic and the Spc110 C-nontoxic cells. In this occasion only, the largest aggregate per cell was used to calculate the fluorescence intensity.

Cdc20 assay

Met-*CDC20*-expressing cells were grown in -MET + 2% Raffinose to an OD600 of 0.2. Once set OD600 was reached, 8 mM methionine was added for 5 h while the cultures were in a shaking incubator at 30°C. The culture was then divided, and half was grown in YEP medium containing 2% raffinose plus 8 mM methionine media, and 2% galactose was added to the other half for 3 h at 30°C. Samples of the cells were fixed with 4% formaldehyde in 100 mM sucrose and imaged.

Immuno-EM

Yeast cultures were prepared for immuno-EM as described previously (Giddings *et al.*, 2001). Cells overexpressing the Spc110 AA741–944 C terminal fragment (Spc110 C-toxic) or the Spc110 AA741–923 C terminal fragment (Spc110 C-nontoxic) were grown overnight at 30°C in synthetic media lacking uracil and containing 2% raffinose. Cells were diluted to an OD600 of 0.2 and grown for 3 h in 2% galactose medium to induce the expression of the constructs. After induction, the cells were high-pressure frozen in a Wohlwend Compact 02 HPF, freeze-substituted in 0.25% glutaraldehyde, 0.1% uranyl acetate in acetone, and embedded in Lowicryl HM20. Thin serial sections were poststained in uranyl acetate and lead citrate and imaged in a transmission electron microscope (FEI Phillips CM100 electron microscope). Serial thin sections were then immuno-labeled with a rabbit anti-GFP polyclonal antibody provided by Chad Pearson (University of Colorado Anschutz Medical Campus).

Yeast two-hybrid analysis

Yeast two-hybrid analysis was conducted by amplifying SPC29 and SPC42 from yeast genomic DNA with *Bam*HI and *Sal*I ends and ligated them into pMW2891/GBDU-C1. To generate the series of Spc110 C terminal fragments fused to the GAL4-AD, Spc110 C

terminal fragments were synthesized by PCR with terminal *Bam*HI and *Sal*I restriction sites using plasmid DNA from pMW2661. These products were cloned into the *Bam*HI and *Sal*I restriction sites of p2888/GAD-C1 (Table 1). These clones were sequenced and confirmed to lack PCR-induced mutations. Plasmids were cotransformed into yMW5227 (PJ69-4α) (James *et al.*, 1996). Transformants were selected on plates lacking uracil and leucine (-URA, -LEU). Protein interactions were tested on plates lacking histidine (-HIS). In some instances, 3-AT (3-amino-1,2,4-triazole, Sigma-Aldrich) was added at 1–30 mM to reduce background growth. Plates were incubated at 30°C for 3 d.

Lysate preparation and immunoblotting

Protein samples were prepared from strains overexpressing the toxic Spc110 C-toxic fragment or the Spc110 C-nontoxic fragment. Strains were grown to midexponential phase to an OD600 of 0.2 in YEP + 2% raffinose media. The constructs were induced with 2% galactose for 3 h at 30°C. Cells were collected by low-speed centrifugation, washed, and resuspended in B150 breaking buffer containing 1 mM phenylmethylsulfonyl fluoride, 20 mM N-ethylmaleimide, and 1% Sigma-Aldrich protease inhibitor. Cells were lysed by vortexing with glass beads for 10 min at 4°C. Extracts were clarified by centrifugation at 14,000 × *g* for 20 min at 4°C. Samples were run in an 8% SDS–PAGE gel. Protein concentrations were determined by Bradford Protein Assay (Bio-Rad) using bovine serum albumin as the standard. The membrane was blocked in 0.2% Tropix I-block reagent (Applied Biosystems) with 0.1% Tween-20 in PBS overnight at 4°C. The GFP tag was detected using a mouse monoclonal anti-GFP antibody (Biolegend).

ACKNOWLEDGMENTS

We thank Sue Jaspersen for the Pus1-mCherry strain and for her technical support. We also thank Michele Jones for her technical support and for her review and editing of this manuscript. A.A. was supported by NIH T32 Oncogenic Signals and Chromosome Biology Training grant (T32 CA 108459). This work was also supported by the NIH (GM105537 to M.W.). EM analysis was carried out by the CU-Boulder Electron Microscopy facility.

REFERENCES

Adams IR, Kilmartin JV (1999). Localization of core spindle pole body (SPB) components during SPB duplication in Saccharomyces cerevisiae. J Cell Biol 145, 809–823.

Azimzadeh J, Bornens M (2007). Structure and duplication of the centrosome. J Cell Sci 120, 2139–2142.

Bornens M (2012). The centrosome in cells and organisms. Science 335, 422–426.

Brachat A, Kilmartin JV, Wach A, Philippsen P (1998). Saccharomyces cerevisiae cells with defective spindle pole body outer plaques accomplish nuclear migration via half-bridge-organized microtubules. Mol Biol Cell 9, 977–991.

Byers B, Goetsch L (1974). Duplication of spindle plaques and integration of the yeast cell cycle. Cold Spring Harb Symp Quant Biol 38, 123–131.

Byers B, Goetsch L (1975). Behavior of spindles and spindle plaques in the cell cycle and conjugation of Saccharomyces cerevisiae. J Bacteriol 124, 511–523.

Delaval B, Doxsey SJ (2010). Pericentrin in cellular function and disease. J Cell Biol 188, 181–190.

Doxsey SJ, Stein P, Evans L, Calarco PD, Kirschner M (1994). Pericentrin, a highly conserved centrosome protein involved in microtubule organization. Cell 76, 639–650.

Elliott S, Knop M, Schlenstedt G, Schiebel E (1999). Spc29p is a component of the Spc110p subcomplex and is essential for spindle pole body duplication. Proc Natl Acad Sci USA 96, 6205–6210.

Flick JS, Johnston M (1990). Two systems of glucose repression of the GAL1 promoter in Saccharomyces cerevisiae. Mol Cell Biol 10, 4757–4769.

Flory MR, Morphew M, Joseph JD, Means AR, Davis TN (2002). Pcp1p, an Spc110p-related calmodulin target at the centrosome of the fission yeast Schizosaccharomyces pombe. Cell Growth Differ 13, 47–58.

Flory MR, Moser MJ, Monnat RJ Jr, Davis TN (2000). Identification of a human centrosomal calmodulin-binding protein that shares homology with pericentrin. Proc Natl Acad Sci USA 97, 5919–5923.

Fong KK, Sarangapani KK, Yusko EC, Riffle M, Llauro A, Graczyk B, Davis TN, Asbury CL (2017). Direct measurement of the strength of microtubule attachment to yeast centrosomes. Mol Biol Cell 28, 1853–1861.

Friederichs JM, Ghosh S, Smoyer CJ, McCroskey S, Miller BD, Weaver KJ, Delventhal KM, Unruh J, Slaughter BD, Jaspersen SL (2011). The SUN protein Mps3 is required for spindle pole body insertion into the nuclear membrane and nuclear envelope homeostasis. PLoS Genet 7, e1002365.

Ganem NJ, Godinho SA, Pellman D (2009). A mechanism linking extra centrosomes to chromosomal instability. Nature 460, 278–282.

Gardner JM, Jaspersen SL (2014). Manipulating the yeast genome: deletion, mutation, and tagging by PCR. Methods Mol Biol 1205, 45–78.

Geier BM, Wiech H, Schiebel E (1996). Binding of centrins and yeast calmodulin to synthetic peptides corresponding to binding sites in the spindle pole body components Kar1p and Spc110p. J Biol Chem 271, 28366–28374.

Geiser JR, Sundberg HA, Chang BH, Muller EG, Davis TN (1993). The essential mitotic target of calmodulin is the 110-kilodalton component of the spindle pole body in Saccharomyces cerevisiae. Mol Cell Biol 13, 7913–7924.

Geiser JR, van Tuinen D, Brockerhoff SE, Neff MM, Davis TN (1991). Can calmodulin function without binding calcium? Cell 65, 949–959.

Giddings TH Jr, O'Toole ET, Morphew M, Mastronarde DN, McIntosh JR, Winey M (2001). Using rapid freeze and freeze-substitution for the preparation of yeast cells for electron microscopy and three-dimensional analysis. Methods Cell Biol 67, 27–42.

Gillingham AK, Munro S (2000). The PACT domain, a conserved centrosomal targeting motif in the coiled-coil proteins AKAP450 and pericentrin. EMBO Rep 1, 524–529.

Goh PY, Kilmartin JV (1993). NDC10: a gene involved in chromosome segregation in Saccharomyces cerevisiae. J Cell Biol 121, 503–512.

Gordon O, Taxis C, Keller PJ, Benjak A, Stelzer EH, Simchen G, Knop M (2006). Nud1p, the yeast homolog of Centriolin, regulates spindle pole body inheritance in meiosis. EMBO J 25, 3856–3868.

Ito D, Bettencourt-Dias M (2018). Centrosome remodelling in evolution. Cells 7.

Ito T, Chiba T, Ozawa R, Yoshida M, Hattori M, Sakaki Y (2001). A comprehensive two-hybrid analysis to explore the yeast protein interactome. Proc Natl Acad Sci USA 98, 4569–4574.

James P, Halladay J, Craig EA (1996). Genomic libraries and a host strain designed for highly efficient two-hybrid selection in yeast. Genetics 144, 1425–1436.

Jaspersen SL, Winey M (2004). The budding yeast spindle pole body: structure, duplication, and function. Annu Rev Cell Dev Biol 20, 1–28.

Jones MH, Keck JM, Wong CC, Xu T, Yates JR 3rd, Winey M (2011). Cell cycle phosphorylation of mitotic exit network (MEN) proteins. Cell Cycle 10, 3435–3440.

Kilmartin JV (2003). Sfi1p has conserved centrin-binding sites and an essential function in budding yeast spindle pole body duplication. J Cell Biol 162, 1211–1221.

Kilmartin JV (2014). Lessons from yeast: the spindle pole body and the centrosome. Philos Trans R Soc Lond B Biol Sci 369.

Kilmartin JV, Dyos SL, Kershaw D, Finch JT (1993). A spacer protein in the Saccharomyces cerevisiae spindle poly body whose transcript is cell cycle-regulated. J Cell Biol 123, 1175–1184.

Kilmartin JV, Goh PY (1996). Spc110p: assembly properties and role in the connection of nuclear microtubules to the yeast spindle pole body. EMBO J 15, 4592–4602.

Knop M, Pereira G, Geissler S, Grein K, Schiebel E (1997). The spindle pole body component Spc97p interacts with the gamma-tubulin of Saccharomyces cerevisiae and functions in microtubule organization and spindle pole body duplication. EMBO J 16, 1550–1564.

Knop M, Schiebel E (1997). Spc98p and Spc97p of the yeast gamma-tubulin complex mediate binding to the spindle pole body via their interaction with Spc110p. EMBO J 16, 6985–6995.

Knop M, Schiebel E (1998). Receptors determine the cellular localization of a gamma-tubulin complex and thereby the site of microtubule formation. EMBO J 17, 3952–3967.

Kollman JM, Merdes A, Mourey L, Agard DA (2011). Microtubule nucleation by gamma-tubulin complexes. Nat Rev Mol Cell Biol 12, 709–721.

Lau CK, Giddings TH Jr, Winey M (2004). A novel allele of Saccharomyces cerevisiae NDC1 reveals a potential role for the spindle pole body component Ndc1p in nuclear pore assembly. Eukaryot Cell 3, 447–458.
Lengauer C, Kinzler KW, Vogelstein B (1998). Genetic instabilities in human cancers. Nature 396, 643–649.
Lin TC, Neuner A, Schlosser YT, Scharf AN, Weber L, Schiebel E (2014). Cell-cycle dependent phosphorylation of yeast pericentrin regulates gamma-TuSC-mediated microtubule nucleation. Elife 3, e02208.
Longtine MS, McKenzie A 3rd, Demarini DJ, Shah NG, Wach A, Brachat A, Philippsen P, Pringle JR (1998). Additional modules for versatile and economical PCR-based gene deletion and modification in Saccharomyces cerevisiae. Yeast 14, 953–961.
Mahen R, Venkitaraman AR (2012). Pattern formation in centrosome assembly. Curr Opin Cell Biol 24, 14–23.
Morais MC, Kanamaru S, Badasso MO, Koti JS, Owen BA, McMurray CT, Anderson DL, Rossmann MG (2003). Bacteriophage phi29 scaffolding protein gp7 before after prohead assembly. Nat Struct Biol 10, 572–576.
Muller EG, Snydsman BE, Novik I, Hailey DW, Gestaut DR, Niemann CA, O'Toole ET, Giddings TH Jr, Sundin BA, Davis TN (2005). The organization of the core proteins of the yeast spindle pole body. Mol Biol Cell 16, 3341–3352.
Murphy SM, Urbani L, Stearns T (1998). The mammalian gamma-tubulin complex contains homologues of the yeast spindle pole body components spc97p and spc98p. J Cell Biol 141, 663–674.
Nguyen T, Vinh DB, Crawford DK, Davis TN (1998). A genetic analysis of interactions with Spc110p reveals distinct functions of Spc97p and Spc98p, components of the yeast gamma-tubulin complex. Mol Biol Cell 9, 2201–2216.
O'Toole ET, Mastronarde DN, Giddings TH Jr, Winey M, Burke DJ, McIntosh JR (1997). Three-dimensional analysis and ultrastructural design of mitotic spindles from the cdc20 mutant of Saccharomyces cerevisiae. Mol Biol Cell 8, 1–11.
O'Toole ET, Winey M, McIntosh JR (1999). High-voltage electron tomography of spindle pole bodies and early mitotic spindles in the yeast Saccharomyces cerevisiae. Mol Biol Cell 10, 2017–2031.
Oakley CE, Oakley BR (1989). Identification of gamma-tubulin, a new member of the tubulin superfamily encoded by mipA gene of Aspergillus nidulans. Nature 338, 662–664.
Pihan GA, Purohit A, Wallace J, Knecht H, Woda B, Quesenberry P, Doxsey SJ (1998). Centrosome defects and genetic instability in malignant tumors. Cancer Res 58, 3974–3985.
Rieder CL, Faruki S, Khodjakov A (2001). The centrosome in vertebrates: more than a microtubule-organizing center. Trends Cell Biol 11, 413–419.
Rout MP, Kilmartin JV (1990). Components of the yeast spindle and spindle pole body. J Cell Biol 111, 1913–1927.
Ruthnick D, Schiebel E (2016). Duplication of the yeast spindle pole body once per cell cycle. Mol Cell Biol 36, 1324–1331.
Schramm C, Elliott S, Shevchenko A, Schiebel E (2000). The Bbp1p-Mps2p complex connects the SPB to the nuclear envelope and is essential for SPB duplication. EMBO J 19, 421–433.
Sibanda BL, Critchlow SE, Begun J, Pei XY, Jackson SP, Blundell TL, Pellegrini L (2001). Crystal structure of an Xrcc4-DNA ligase IV complex. Nat Struct Biol 8, 1015–1019.
Smoyer CJ, Katta SS, Gardner JM, Stoltz L, McCroskey S, Bradford WD, McClain M, Smith SE, Slaughter BD, Unruh JR, *et al.* (2016). Analysis of membrane proteins localizing to the inner nuclear envelope in living cells. J Cell Biol 215, 575–590.
Stirling DA, Rayner TF, Prescott AR, Stark MJ (1996). Mutations which block the binding of calmodulin to Spc110p cause multiple mitotic defects. J Cell Sci 109, 1297–1310.
Stirling DA, Stark MJ (2000). Mutations in SPC110, encoding the yeast spindle pole body calmodulin-binding protein, cause defects in cell integrity as well as spindle formation. Biochim Biophys Acta 1499, 85–100.
Stirling DA, Welch KA, Stark MJ (1994). Interaction with calmodulin is required for the function of Spc110p, an essential component of the yeast spindle pole body. EMBO J 13, 4329–4342.
Strnad P, Gonczy P (2008). Mechanisms of procentriole formation. Trends Cell Biol 18, 389–396.
Surana U, Liang H, Lim HH (2012). Staging a recovery from mitotic arrest: Unusual ways of Cdk1. Bioarchitecture 2, 33–37.
Vinh DB, Kern JW, Hancock WO, Howard J, Davis TN (2002). Reconstitution and characterization of budding yeast gamma-tubulin complex. Mol Biol Cell 13, 1144–1157.
Viswanath S, Bonomi M, Kim SJ, Klenchin VA, Taylor KC, Yabut KC, Umbreit NT, Van Epps HA, Meehl J, Jones MH, *et al.* (2017). The molecular architecture of the yeast spindle pole body core determined by Bayesian integrative modeling. Mol Biol Cell 28, 3298–3314.
Winey M, Goetsch L, Baum P, Byers B (1991). MPS1 and MPS2: novel yeast genes defining distinct steps of spindle pole body duplication. J Cell Biol 114, 745–754.
Winey M, Hoyt MA, Chan C, Goetsch L, Botstein D, Byers B (1993). NDC1: a nuclear periphery component required for yeast spindle pole body duplication. J Cell Biol 122, 743–751.
Winey M, Mamay CL, O'Toole ET, Mastronarde DN, Giddings TH Jr, McDonald KL, McIntosh JR (1995). Three-dimensional ultrastructural analysis of the Saccharomyces cerevisiae mitotic spindle. J Cell Biol 129, 1601–1615.
Winey M, O'Toole ET (2001). The spindle cycle in budding yeast. Nat Cell Biol 3, E23–E27.
Yoder TJ, McElwain MA, Francis SE, Bagley J, Muller EG, Pak B, O'Toole ET, Winey M, Davis TN (2005). Analysis of a spindle pole body mutant reveals a defect in biorientation and illuminates spindle forces. Mol Biol Cell 16, 141–152.
Yoder TJ, Pearson CG, Bloom K, Davis TN (2003). The Saccharomyces cerevisiae spindle pole body is a dynamic structure. Mol Biol Cell 14, 3494–3505.
Zachariae W, Nasmyth K (1999). Whose end is destruction: cell division and the anaphase-promoting complex. Genes Dev 13, 2039–2058.
Zheng Y, Wong ML, Alberts B, Mitchison T (1995). Nucleation of microtubule assembly by a gamma-tubulin-containing ring complex. Nature 378, 578–583.